Controlling Flows in Microchannels with Patterned Surface Charge and Topography

ABRAHAM D. STROOCK AND
GEORGE M. WHITESIDES*
Department of Chemistry and Chemical Biology, Harvard University, Cambridge, Massachusetts 02138

Received December 30, 2002

ABSTRACT
This Account reviews two procedures for controlling the flow of fluids in microchannels. The first procedure involves patterning the density of charge on the inner surfaces of a channel. These patterns generate recirculating electroosmotic flows in the presence of a steady electric field. The second procedure involves patterning topography on an inner surface of a channel. These patterns generate recirculation in the cross-section of steady, pressure-driven flows. This Account summarizes applications of these flow to mixing and to controlling dispersion (band broadening).

Introduction

Work in the field of microfluidics has been stimulated over the past decade largely by applications in analytical[1] and bioanalytical chemistry,[2−4] and in high-throughput synthesis and screening;[5] microfluidic systems have also been developed as tools for fundamental research.[6,7] These applications require controlling the flow of liquids in channels with lateral dimensions of ~100 μm. Examples of manipulations of fluid that are important include the positioning streams within the cross-section of the channel for the precise delivery of regents, the mixing of solutions required for chemical reactions, and the transportation of small volumes (<1 μL) of solution for high-throughput syntheses and analyses. Ideally, the designs of fluidic components for these tasks should be compatible with common planar microfabrication techniques,[8,9] inexpensive to fabricate, simple to operate, appropriate for the physical characteristics of flows of liquids in microchannels, and insensitive to variations in the composition of the fluid.

This Account reviews two strategies that we have pursued to control the local form—direction and magnitude—of flows in microchannels. Both approaches involve creating structures—chemical or mechanical—on the inner surfaces of a microchannel such as the one shown schematically in Figure 1A. In the first strategy, we patterned the surface of the channel with alternating bands of positive and negative charge density and applied an electric field along the channel in order to generate electroosmotic (EO) flows (Figure 1B); the form of these EO flows is dictated by the pattern of the charge on the surface. In the second strategy, we patterned the topography of one wall of the channel in the form of grooves that are oriented at oblique angles with respect to the long axis of the channel, and applied a pressure gradient along the channel (Figure 1C); the form of these pressure-driven flows is dictated by the pattern of the grooves. These structured flows—multidirectional flows along the axis of the channel and recirculating flows in the cross-section of the channel—can be used to position streams within the channel, mix streams of miscible fluids, and control dispersion (spreading) of solute along the direction of the flow. These techniques of patterning flows operate passively, that is, with no moving parts or time-dependent electric fields or pressure gradients. The systems that we describe were fabricated using soft lithographic methods in poly(dimethylsiloxane) (PDMS) and glass.[9,10]

We organize this Account into three sections. In the first, we give a brief overview of the technical and physicochemical aspects of microfluidics, of the general characteristics of EO and pressure-driven flows, and of the different strategies that we and others have pursued to control flows in the microfluidic systems. In the second, we mention methods for controlling the density of charge on surfaces, and review our results on patterning EO flows

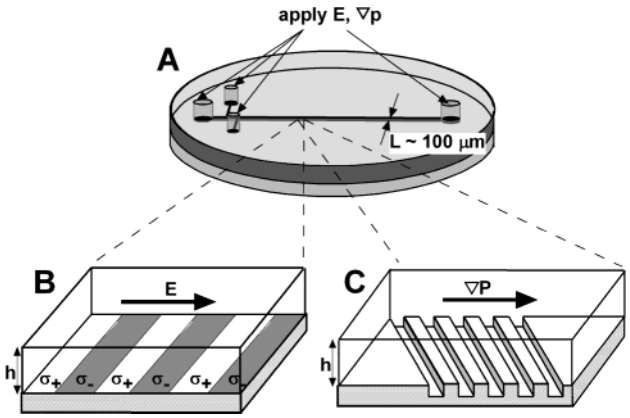

FIGURE 1. Strategies for controlling flows in microchannels. (A) Scheme showing the typical format of a microfluidic channel. The arrows indicate reservoirs at which samples are introduced and removed, and electric fields and pressure gradients are applied. (B) Patterned electroosmotic flow. Scheme showing a section of microchannel in which the density of charge, σ, on the floor is patterned into positive (σ_+) and negative (σ_-) bands. (C) Patterned pressure-driven flows. Scheme showing a section of microchannel with a pattern of grooves on the floor.

Abraham D. Stroock was born in Boulder, CO, in 1973. He received his B.A. degree from Cornell University in 1995 and his Ph.D. degree with George M. Whitesides from Harvard University in 2002. He is presently an assistant professor of Chemical and Biomolecular Engineering at Cornell University. His research interests include fluid-based microsystems, colloidal self-assembly, and interfacial phenomena.

George M. Whitesides was born in Lexington, KY, in 1939. He received his A.B. degree from Harvard University in 1960 and his Ph.D. degree with John D. Roberts from the California Institute of Technology in 1964. He was a member of the faculty of the Massachusetts Institute of Technology from 1963 to 1982. He joined the Department of Chemistry at Harvard University in 1982, where he is now the Mallinckrodt Professor of Chemistry. His research interests include microfabrication, materials science, surface chemistry, self-assembly, rational drug design, and molecular recognition.

* To whom correspondence should be addressed. Telephone: (617) 495-9430. Telefax: (617) 495-9857. E-mail: gwhitesides@gmwgroup.harvard.edu.

10.1021/ar0202870 CCC: $25.00 © 2003 American Chemical Society
Published on Web 05/17/2003

Table 1. Comparison of Electroosmotic and Pressure Driven Flow

electroosmotic flow	pressure-driven flow
• no moving parts (+)	• often moving parts (−)
• uniform flow profile ⇒ bands of solute with the same electrophoretic mobility broaden only by diffusion (+)	• parabolic flow profile ⇒ bands of a solute broaden rapidly due to differences of flow speed over cross-section of channel (−)
• high voltages (>100 V/cm) (−)	• low voltage, gravity, osmosis (+)
• sensitive to surface contamination (−)	• insensitive to surface contamination (+)
• only polar solvents (−)	• any solvent (+)
• low flow speeds (<1 mm/s) (−)	• wide range of flow speeds (<100 cm/s) (+)
• separation of mixtures by charge-to-size ratio (+ for analysis, − for general transport)	• no separation (−)

with patterned charge. In the third section, we mention methods of patterning topography inside of microchannels, describe the interaction of pressure-driven flows with topography, and review our results on patterning pressure-driven flows with patterns of grooves. In this third section, we also describe a chaotic mixer that is based on the patterning of pressure-driven flows and show how this mixer can be used to control the broadening of bands of solute as they travel in pressure-driven flows. We comment on the strengths and weaknesses of both the EO and the pressure-driven strategies.

I. Overview of Flows in Microchannels

Technical Context. Among the desired characteristics of microfluidic systems are (1) portability and appropriateness for field-use, (2) the ability to control and process small volumes ($\leq$ 1 μL) of fluid, (3) the potential to integrate complex, fluid based processes with electronic and optical hardware, and (4) the improvement of the speed of processes relative to that in conventional, benchtop devices. To achieve these characteristics, certain constraints on the design and fabrication of microfluidic systems must be considered. In particular, the need for small elements (e.g., channels with cross-sectional dimensions of 10−1000 μm) with potential to interface with integrated electronics has led to the use of planar fabrication methods that have been adapted from the microelectronics industry.[2,8,11] The need for portability and field-use calls for durability and simplicity of operation. For applications in bioanalysis, disposable devices are desirable, and the cost of fabrication should be low. The techniques for manipulating flows that are reviewed in this Account satisfy many of these constraints: the required mechanical and chemical patterns can all be fabricated using soft lithographic methods that are inexpensive, widely accessible, and compatible with the integration of electronic and optical elements.[11−15] The passive nature of operation of these techniques is attractive for field use.

Physicochemical Context. In microchannels, flows of common liquids driven by typical electric fields ($\sim$ 100 V/cm) and pressure gradients (<1 bar/cm), are characterized by low values of the Reynolds number (Re < 100).[16] For these values of Re, flows are laminar (i.e., not turbulent), and inertial effects, such as the eddies that form downstream of an obstruction in the flow, are weak. In laminar flows, the motion of solute across the direction of the flow is due only to molecular diffusion. The lack of convective transport (i.e., motion with the flow) of solute across the flow means that homogenization of chemical species across channels with 100 μm dimensions can take many seconds to minutes;[17,18] this mixing time could be the rate-limiting step for chemical applications. We also note that, on the size scale of microchannels, the characteristics of the inner surfaces of the channel—density of charge, topography, and wettibility—can have large effects on the flow in the bulk of the fluid.

Electroosmotic Flow in Simple Channels. The surfaces of many materials become electrostatically charged when placed in contact with polar solvents; the compensating charge resides in a layer of fluid adjacent to the charged surface; this layer is referred to as the Debye screening layer. In common aqueous buffers, the thickness of the Debye layer, λ_D, is less than 10 nm.[19] When an electric field is applied along a channel that is filled with a polar solvent, an electroosmotic flow is generated by the net force that is exerted by the field on the mobile charges in the Debye layer at the walls of the channel. In a uniformly charged channel, the fluid outside the Debye layer (i.e., in the bulk of the fluid) is carried at a uniform speed by the motion of the fluid inside the Debye layer. The flow is uniaxial along the axis of the channel with velocity $U_{EO} = (\sigma\lambda_D/\eta)E = \mu_{eo}E$, where σ (C/cm^2) is the surface charge density, η (g/(cm s)) is the dynamic viscosity of the fluid, E (V/cm) is the component of the applied field parallel to the walls, and μ_{eo} ((cm/s)/(V/cm)) is the EO mobility of the surface.[19,20] Table 1 summarizes characteristics of EO flows.

Pressure-Driven Flow in Simple Channels. When a pressure gradient is maintained along a channel, pressure-driven flow, termed Poiseuille flow, is generated in the opposing direction (i.e., from high pressure to low pressure). At low Re, the flow is uniaxial along the principal axis of the channel, and speed of the flow varies in parabolic manner over the cross-section of the channel; the speed is zero at the walls and maximum in the center of the channel. This variation of speed over the cross-section leads to rapid dispersion (broadening) of bands of solute in the flow; the volume of fluid occupied by the solute is stretched along the flow as the portion of the volume near the center of the channel outpaces the portion near the walls.[21] Table 1 summarizes characteristics of pressure-driven flows.

Strategies for Controlling Flows in Microchannels. Table 2 presents a nonexhaustive list of techniques that have been used for manipulating flows in microchannels.

Table 2. Strategies for Controlling Flows in Microchannels

strategy for controlling flow	applications	reference
patterned surface charge (EO)	controlling dispersion	20, 24, 25, 30, 33−35
patterned topography (pressure and EO)	mixing, controlling dispersion	20, 36−39
three-dimensional channels (pressure)	mixing	40
magnetohydrodynamics	pumping, mixing	41−43
patterned wettibility (pressure)	pumping, valving	44, 45
peristalsis (pressure)	pumping, valving	12, 46
patterned electrodes (EO)	pumping	47−49

A more complete review of techniques can be found in recent reviews by the group of Andreas Manz.[22,23] The techniques listed in Table 2 have the common characteristic that they involve the addition of structure along the length of the channel in the form of chemical modification, topography, intersecting channels, or electrodes. The flows generated by these techniques can be roughly separated into two categories: i) those with transverse components that are useful for mixing and for controlling dispersion (treated in this Account), and ii) those with net motion along the channel that are useful as pumps.

II. Patterning Electroosmotic Flow

Controlling Density of Charge on the Surfaces of Microchannels. Manipulation of EO flows requires the ability to control the density of charge on surfaces. We[24] and others[25] have used the adsorption of poly(electrolyte) multilayers[26] to modify the surface charge density on the walls of micrchannels. The surface charge changes sign with each additional layer, such that the EO mobility, $\mu_{eo} \sim \pm 3-4$ (μm/s)/(V/cm) ($\mu_{eo} \sim -6$ (μm/s/(V/cm)) on glass).[24,25] Others have demonstrated a variety of other techniques for controlling the density of charge on surfaces both passively[27−30] and actively.[31,32]

Patterning EO Flows. We considered two types of patterns of charge: one in which regions of positive and negative density of charge extend along the axis of the channel and the direction of the applied field (diagram in Figure 2A), and the other in which the regions of positive and negative density of charge extend across the channel and the applied field (diagram in Figure 2B). The flows generated in these two geometries represent the principal types of flows that are expected for any distribution of charge on channel walls.[33] Due to the linearity of fluid dynamics at low Re, models for the EO flow in the presence of general distributions of charge can be formed from linear superpositions of simple patterns such as the ones that we considered.

We generated the first type of pattern (Figure 2A) by laminar flow patterning[50,51] of poly(electrolyte) layers. As is shown schematically on the top and in the trajectories of tracer beads on the bottom in Figure 2A, the flow was bi-directional along the channel; the fluid moved in the direction of E on the negative side of the channel (positive Debye layer), and the fluid moved in the opposite direction from E on the positive side of the channel (negative Debye layer). This flow was the same as the shear flow that would be generated by mechanically moving the two halves of the channel in opposite directions. This type of multidirectional flow of a single fluid would be difficult to achieve in a channel with globally applied pressures. We note though that Zhao et al. have demonstrated bidirectional flow of immiscible liquids in a microchannel.[52] The second type of pattern (Figure 2B) was generated in two steps: (i) A glass slide was patterned with bands of positive and negative charge using vacuum assisted micromolding in capillaries,[53] and (ii) this glass slide was used as the fourth wall of a channel structure in a slab of PDMS. With the bands of charge extended across the channel, the applied field pulled the fluid in opposite directions over adjacent regions of the patterned wall. The fluid behaved as if adjacent regions of the walls were mechanically moving in opposite directions. This motion at the boundary created alternating regions of high and low pressure at the interfaces between bands, and the fluid recirculated in the direction normal to the wall. The resulting cellular flow is seen in the trajectories of tracer beads in Figure 2B. This cellular flow is reminiscent of thermally driven convection. Generating a sufficient temperature gradient to generate these flows thermally would be difficult on the micron-scale. We also note that generating these two types of flows with mechanical motion (i.e., sliding walls) would not be practical with current microfabrication technology. We successfully modeled both of these flows analytically.[24]

Other Applications of Patterned EO Flow. Mixing is another potential application of patterned EO flows. Erickson and Li have modeled mixing in recirculating EO flows such as those in Figure 2B.[35] Johnson et al. have demonstrated mixing in EO flows in channels with a combination of patterned surface charge density and grooves on the floor of the channel.[37] Johnson et al. have also used patterned charge to reduce the broadening of bands of solute driven by EO flow though bends in microchannels.[30] Panwar and Kumar have study the possibility of manipulating the position and conformation of polymers in patterned EO flows.[54]

III. Patterning Pressure-Driven Flows

Patterning Grooves in Microchannels. Obliquely oriented grooves on one wall of a microchannel are sufficient to generate transverse components in pressure-driven flows (Figure 3A).[39] These groove-structures are easily fabricated using planar lithographic methods. To fabricate the channels in PDMS, we made master structures in a photocurable epoxy resist with two layers of photolithography, and molded these structures in PDMS.[55] In making the master, the first layer of photolithography defined a positive image of our channel structure; the second layer defined a positive image of the pattern of grooves. The

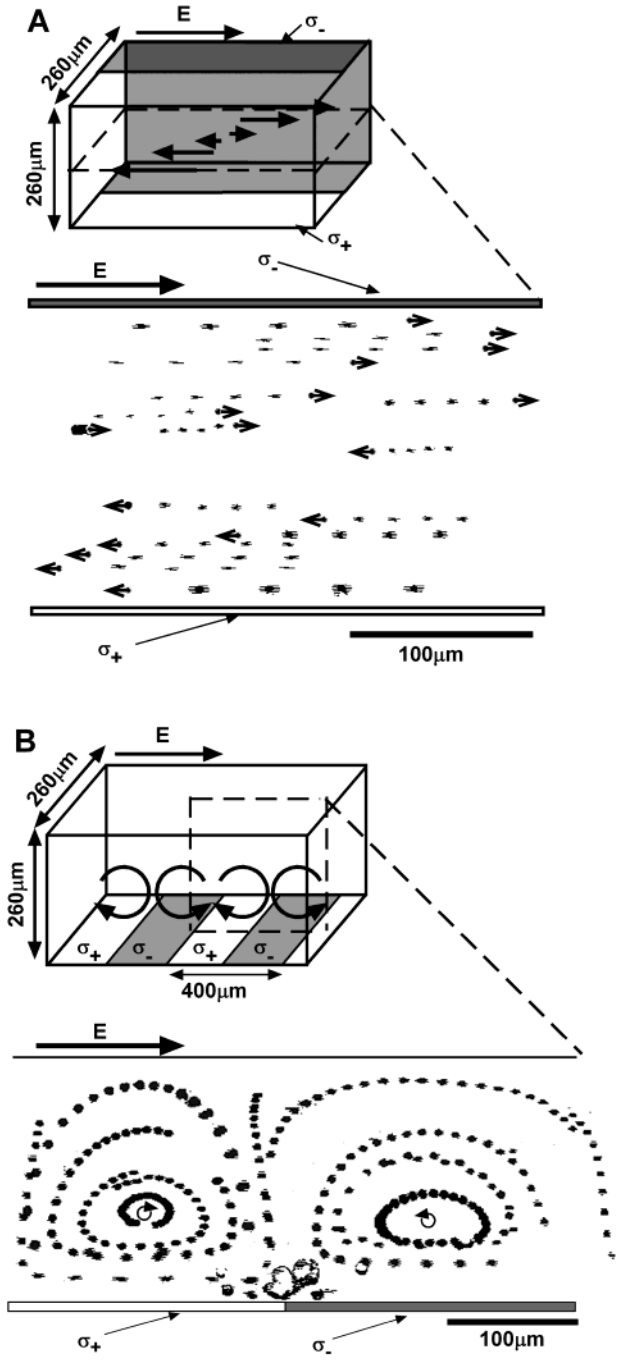

FIGURE 2. Patterned electroosmotic flow. The schemes at the tops of both panels A and B show the patterns of density of charge that we considered. The EO flows in these geometries are shown schematically with arrows. At the bottom of both frames are micrographs that show the trajectories of fluorescent beads in a plane (horizontal in panel A and vertical in panel B) through the channel as shown in the schematic diagrams. The micrographs were compiled from multiple series of images that were taken at intervals of 0.2 s. The direction of motion is indicated by arrows. In both experiments, the applied electric field was, $E = 95$ V/cm. In panel B, the globular objects at the bottom of the image are beads that have stuck to the surface at the stagnation point in the flow at the transition between positively and negatively charged regions. Adapted from Stroock et al.[24]

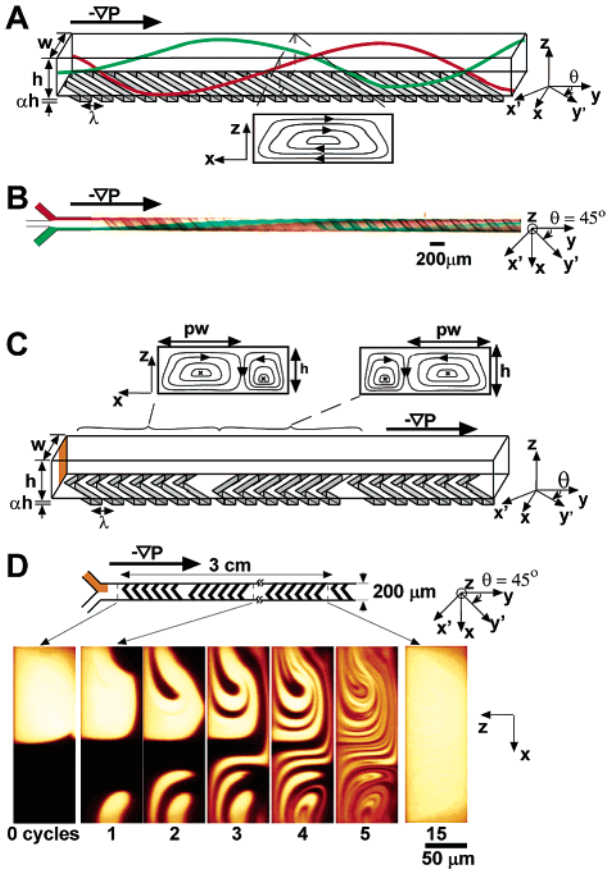

FIGURE 3. Patterned pressure-driven flow. (A) Scheme showing a section of channel with a regular series of grooves in the floor that are oriented at a oblique angle, θ, with respect to the principal axis of the channel. The helical form of two trajectories in a pressure-driven flow in this channel are shown schematically with the red and green lines. The average, recirculating flow in the cross-section is shown schematically below the channel. The principal axes of the channel are (x, y, z) and the principal axes of the grooves are (x', y', z). (B) Optical micrograph of a red, a clear, and a green stream flowing through a channel such as the one in panel A. The three inlets are drawn schematically on the left. In this channel, $\theta = 45°$, the period of the grooves, $\lambda = 200$ μm, the average height of the channel, $h = 70$ μm, the width of the channel, $w = 200$ μm, and the relative depth of the grooves, $\alpha = 0.2$. (C) Scheme showing a section of channel with grooves in the form of the staggered herringbone mixer (SHM) in the floor. One and a half cycles of the mixer are shown. Each half cycle is made up of a regular series of grooves (6 in the case shown) in the form of asymmetrical herringbones; the direction of asymmetry changes from one-half-cycle to the next. The schematic drawings above the channel show the form of the average flow in the cross-section for each half-cycle. (D) Fluorescent confocal micrographs that show the evolution of a stream of fluorescent solution (top) that was injected alongside a stream of clear solution (bottom) in a channel with the SHM as in (C). The micrographs show vertical cross-sections of the channel before the first cycle of the mixer (0 cycles) and after 1, 2, 3, 4, 5, and 15 cycles. In this channel, $\theta = 45°$, $\lambda = 100$ μm, $h = 70$ μm, $w = 200$ μm, $\alpha = 0.18$, and there were 6 grooves per half-cycle. Re $= 10^{-2}$. $D = 2 \times 10^{-8}$ (cm^2/s), and the average speed $U_a = 2$ cm/s. Adapted from Stroock et al.[38]

pattern of grooves was aligned to lie on top of the channel structure in the first layer. We note that this type of two-level structure can also be fabricated with conventional photolithographic procedures that involve spatially selective etching of silicon and glass.[8]

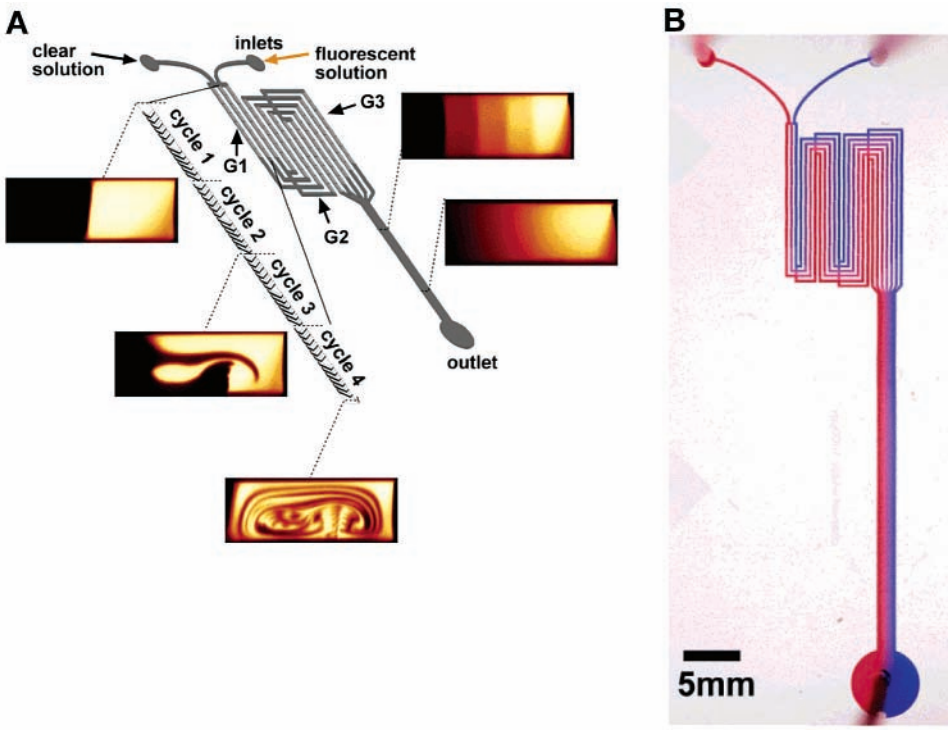

FIGURE 4. Gradient mixer that incorporates the SHM design. (A) Scheme of a network of microfluidic channels into which two streams of different composition are injected and out of which a single stream with a smooth linear gradient between the compositions of the input solutions is recovered. The network shown has three generations (G1, G2, and G3). Confocal micrographs show the distribution of fluorescence from a solution of fluorescein that was injected into the inlet on the right. (B) Optical micrograph of a network such as the one in panel A, into which a solution of red dye (left) and a solution of blue dye (right) were injected.

Patterned Flows over Grooves. The form of trajectories in a flow over a uniform pattern of obliquely oriented grooves is shown schematically in Figure 3A. The net effect of the grooves (averaged over a period of the pattern) is the entrainment of fluid near the structured surface along the direction of the grooves (y'); this motion has a component along x that is perpendicular to both the principal axis of the channel and the applied pressure gradient (along y). This transverse motion leads to an opposing transverse pressure gradient which forces the fluid to circulate back across the top of the channel. The resulting flow has a principal, Poiseuille component along the channel, and a recirculating component in the cross-section; the streamlines of the flow are helical. The micrograph in Figure 3B shows how this helical flow can be used to manipulate the positions of streams in the cross-section of the channel.

Staggered Herringbone Mixer. To achieve mixing of laminar flows in a microchannel, regions of recirculation can be positioned in the cross-section of the channel by placing appropriate regions of grooves on one wall. As streams of fluid flow down the channel, they are stirred into one another by these transverse flows. Figure 3C shows a pattern of grooves on the floor of a channel that lead to efficient stirring of fluids flowing laminarly through the channel; we call this design the staggered herringbone mixer (SHM).[38] A volume of fluid flowing in this channel experiences an series of extensional and rotational flows; this type of alternating flow is known to generate efficient stirring.[56]

Figure 3D shows the evolution of a stream of solution of fluorescent dye (fluorescein labeled polymer, MW 250 000 in a mixture of 80% glycerol/ 20% water by weight) and a stream of clear solution (80% glycerol/ 20% water) as they flow through a channel with the SHM. We worked with viscous solutions of glycerol and water ($\eta = 0.67$ (g/(cm s))), to demonstrate that the observed mixing occurred for low Re (Re < 1). The images are confocal micrographs of vertical cross-sections of the channel. For these solutions in the SHM, the mixing length,[57] $\Delta y_m \sim 3$ cm; this corresponds to 15 cycles of the SHM. In a smooth channel of the same dimensions and under the same flow conditions, $\Delta y_m \sim 10$ m.[58] In the SHM, we found that $\Delta y_m \sim \log(U_a)$, whereas in an unmixed Poiseuille flow, $\Delta y_m \sim U_a$, where U_a is the average flow speed.[21] This logarithmic dependence of the mixing length on the flow speed is an indication that the SHM generates chaotic advection.[56,59] In the SHM, the mixing time, $t_m \sim \Delta y_m/U_a$, can be decreased by increasing the speed of the flow. This relation does not hold in an nonmixing channel in flows at low Re.

Figure 4 shows an application of the SHM in a network of microchannels designed to form smooth gradients of concentration. The network transforms 2 input solutions into 5 output solutions that contain intermediate concentrations of solute in the incoming streams. In each generation (G1, G2, G3) of the network, adjacent streams from the previous generation are joined and fully mixed. The use of the SHM in the mixing sections of this network has three advantages relative to allowing the mixing to

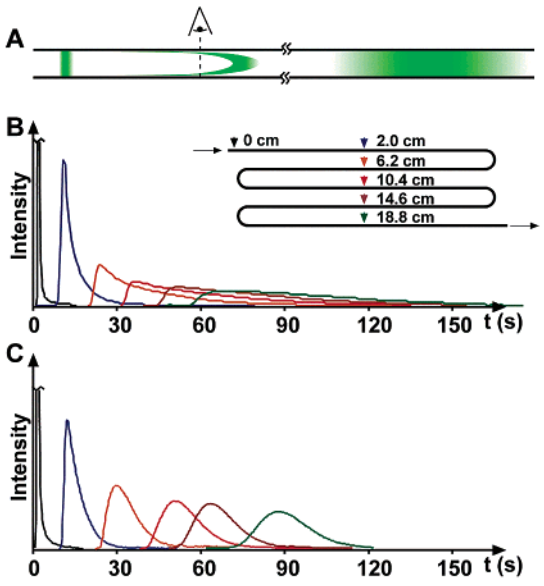

FIGURE 5. Controlling band broadening in pressure-driven flows using the SHM. (A) Schematic drawing showing the evolution of a band of solute in a pressure-driven flow. (B) Unstirred pressure-driven flow in a rectangular channel: $h = 70\ \mu$m, $w = 200\ \mu$m. (C) Stirred pressure-driven flow in a channel with the SHM of the same design as in Figure 3D. In panels B and C, plugs of fluorescent solution were injected into a steady stream of clear solution at the inlet of a channel of the form shown in the inset in (B). The traces in panels B and C represent the fluorescent intensity that was observed as a function of time at different positions along the length of the channel, as indicated in the inset in panel B. The origin of the time axis corresponds to the time of injection for all of the traces. The black traces (0 cm) have been truncated. The dye was fluorescein and the liquid was 80% glycerol/20% water. $D \sim 10^{-7}$ cm^2/s, $U_a \sim 0.1$ cm/s. Adapted from Stroock et al.[38]

occur by diffusion alone, as was done previously:[60] i) the cross-sectional dimension of the channel can be larger; larger channels present lower resistance to flow and are less prone to clogging; ii) the mixing sections can be shorter; and iii) the speed of the flow can be higher.

Control of Dispersion with the SHM. Another application of the SHM is to the control of dispersion in Poiseuille flows in microchannels. As mentioned previously, dispersion occurs in Poiseuille flows because solute in fluid near the middle of the channel moves more rapidly than solute in fluid near the walls. The use of pressure-driven flows for handling μL-scale volumes of solution, and for separations (e.g., by affinity adsorption on the walls) will benefit from a reduction of dispersion. Figure 5A shows schematically the dispersion of a band of solute in a Poiseuille flow. Mixing in the cross-section the flow reduces dispersion relative to an unstirred flow by carrying solute back and forth between the rapidly and slowly moving regions of the flow. Panels B and C of Figure 5 show the evolution of bands of solute as observed as a function of time at different points along the channel. The experiment in Figure 5B was performed in a simple channel; the experiment in Figure 5C was performed in a channel that contained the SHM. In the mixing channel, the bands maintained a larger peak intensity and broadened less than in the simple channel. After 20 cm in the SHM, the bands had dispersed over ~5 cm; this length corresponds to a volume of less than one μL.

Conclusions

The methods that are reviewed in this Account require minimal modifications to the standard geometry (i.e., uniform microchannels) and modes of operations (i.e., steady electric fields and pressure gradients) of microfluidic devices. These simple modifications create qualitatively new fluid behaviors, which can facilitate chemical operations in microsystems. The simplicity and passive nature of these methods make them appropriate for field-use.

These methods of handling fluids may also find applications in more convectional, benchtop systems. For example, the reduction of dispersion with the SHM could be applied in high performance liquid chromatography systems to improve resolution, and reduce the required volume of analyte. For applications in which cost and simplicity of operation are not priorities, active methods of controlling flows may offer advantages relative to the passive methods that we have studied. For example, active mixers have the potential to achieve full mixing in shorter distance than the SHM.[61] We also note that active methods of controlling the density of charge[31,32] and the shape of channels[12] could be used to control in an active manner the types of fluid behavior that we have generated passively.

The ability to pattern flows opens opportunities for new uses of EO and pressure-driven flows in microsystems. With patterns of surface charge density, regions of rotating flow, regions of high and low rates of shear, and stationary points can be positioned with micron-scale precision. These features of the flow could be used to manipulate the position of objects in the flow, generate controlled torques for mechanical actuation, or influence the conformation of macromolecules. By reducing dispersion, the SHM opens the possibility for using pressure-driven flows in a variety of chemical applications. For example, the ability to transport microliter-scale volumes of sample could mean that it is possible to run high-throughput screening and synthesis with molecules in solution (rather than on solid support).

The work Harvard University that is reviewed here was supported by DARPA: NSF ECS-9729405, and NSF: DMR-9809363 MRSEC. We thank Stephan Dertinger for Figure 4.

References

(1) Xu, Y.; Bessoth, F. G.; Eijkel, J. C. T.; Manz, A. On-line monitoring of chromium(III) using a fast micromachined mixer/reactor and chemiluminescence detection. *Analyst* **2000**, *125*, 677−683.
(2) Harrison, D. J.; Fluri, K.; Seiler, K.; Fan, Z.; Effenhauser, C. S.; Manz, A. Micromachining a Miniturized Capillary Electrophoresis-Based Chemical Analysis System on a Chip. *Science* **1993**, *261*, 895−897.
(3) Burns, M. A.; Johnson, B. N.; Brahmasandra, S. N.; Handique, K.; Webster, J. R.; Krishnan, M.; Sammarco, T. S.; Man, P. M.; Jones, D.; Heldsinger, D.; Mastrangelo, C. H.; Burke, D. T. An integrated nanoliter DNA analysis device. *Science* **1998**, *282*, 484−487.

(4) Kopp, M. U.; Mello, A. J. d.; Manz, A. Chemical Amplification: Continuous-Flow PCR on a chip. *Science* **1998**, *280*, 1046−1048.

(5) Mitchell, M. C.; Spikmans, V.; Manz, A.; de Mello, A. J. Microchip-based synthesis and total analysis systems (mu SYNTAS): chemical microprocessing for generation and analysis of compound libraries. *J. Chem. Soc., Perkin Trans. 1* **2001**, 514−518.

(6) Perkins, T.; Smith, D.; Chu, S. Single Polymer Dynamics in Elongational Flow. *Science* **1997**, *276*, 2016−2021.

(7) Takayama, S.; Ostuni, E.; LeDuc, P.; Naruse, K.; Ingber, D. E.; Whitesides, G. M. Laminar flows - Subcellular positioning of small molecules. *Nature* **2001**, *411*, 1016−1016.

(8) Kovacs, G. T. A. *Micromachined Transducers Sourcebook*; WCB/McGraw-Hill: Boston, 1998.

(9) Xia, Y.; Whitesides, G. M. Soft Lithography. *Angew. Chem., Int. Ed. Engl.* **1998**, *37*, 550−575.

(10) McDonald, J. C.; Duffy, D. C.; Anderson, J. R.; Chiu, D. T.; Wu, H.; Schueller, O. J. A.; Whitesides, G. M. Fabrication of microfluidic systems in poly(dimethylsiloxane). *Electrophoresis* **2000**, *21*, 27−40.

(11) Duffy, D. C.; McDonald, J. C.; Schueller, O. J. A.; Whitesides, G. M. Rapid Prototyping of Microfluidic Systems in Poly(dimethylsiloxane). *Anal. Chem.* **1998**, *70*, 4974−4984.

(12) Unger, M. A.; Chou, H.; Thorsen, T.; Scherer, A.; Quake, S. R. Monolithic Microfabricated Valves and Pumps by Multilayer Soft Lithography. *Science* **2000**, *288*, 113−115.

(13) Jo, B. H.; Van Lerberghe, L. M.; Motsegood, K. M.; Beebe, D. J. Three-dimensional micro-channel fabrication in polydimethylsiloxane (PDMS) elastomer. *J. Microelectromech. Syst.* **2000**, *9*, 76−81.

(14) Chabinyc, M. L.; Chiu, D. T.; McDonald, J. C.; Stroock, A. D.; Christian, J. F.; Karger, A. M.; Whitesides, G. M. An Integrated Fluorescence Detection System in Poly(dimethylsiloxane) for Microfluidic Applications. *Anal. Chem.* **2001**, *73*, 4491−4498.

(15) McDonald, J. C.; Whitesides, G. M. Poly(dimethylsiloxane) as a Material for Fabrication of Microfluidic Devices. *Acc. Chem. Res.* **2002**, *35*, 491−499.

(16) $\mathrm{Re} = \rho U_a L/\mu$, where ρ (g/cm^3) is the density of the fluid, U_a (cm/s) is the average flow speed, L (cm) is the typical linear dimension of the system (taken to be the smallest cross-sectional dimension in channels), and μ (g cm^{-1} s^{-1}) is the dynamic viscosity of the fluid. Re is the ratio of the inertial forces to the viscous forces acting on the fluid. Flows are laminar for Re less than ∼2000 in channels.

(17) Bird, R. B.; Stewart, W. E.; Lightfoot, E. N. *Transport Phenomena*, 2nd ed.; John Wiley & Sons: New York, 2002.

(18) The time to diffuse across a channel is $t_D \sim L^2/D$, where L is the typical cross-sectional dimension and D is the diffusivity of the diffusing species. $D = 10^{-5}$ cm^2/s for small molecules to 10^{-7} cm^2/s for proteins. For $L = 100$ μm, $t_D = 10-10^3$ s.[17]

(19) Hunter, R. J. *Foundations of Coilloid Science*; Oxford University Press: New York, 1991.

(20) Ajdari, A. Generation of transverse fluid currents and forces by an electric field: electro-osmosis on charge-modulated and undulated surfaces. *Phys. Rev. E* **1996**, *53*, 4996−5005.

(21) Probstein, R. F. *Physicochemical Hydrodynamics*; Butterworth: Boston, 1989.

(22) Reyes, D. R.; Iossifidis, D.; Auroux, P.-A.; Manz, A. Micro Total Analysis Systems. 1. Introduction, Theory, and Technology. *Anal. Chem.* **2002**, *74*, 2623−2636.

(23) Auroux, P.-A.; Iossifidis, D.; Reyes, D. R.; Manz, A. Micro Total Analysis Systems. 2. Analytical Standard Operations and Applications. *Anal. Chem.* **2002**, *74*, 2637−2652.

(24) Stroock, A. D.; Weck, M.; Chiu, D. T.; Huck, W. T. S.; Kenis, P. J. A.; Ismagilov, R. F.; Whitesides, G. M. Patterning electro-osmotic flow with patterned surface charge. *Phys. Rev. Lett.* **2000**, *84*, 3314−3317. Erratum: *Phys. Rev. Lett.* **2001**, *86*, 6050.

(25) Barker, S. L. R.; Ross, D.; Tarlov, M. J.; Gaitan, M.; Locascio, L. E. Control of flow direction in microfluidic devices with polyelectrolyte multilayers. *Anal. Chem.* **2000**, *72*, 5925−5929.

(26) Decher, G. Fuzzy nanoassemblies: Toward layered polymeric multicomposites. *Science* **1997**, *277*, 1232−1237.

(27) Vanalstine, J. M.; Burns, N. L.; Riggs, J. A.; Holmberg, K.; Harris, J. M. Electrokinetic Characterization of Hydrophilic Polymer-Coatings of Biotechnical Significance. *Colloids Surf., A* **1993**, *77*, 149−158.

(28) Smith, J. T.; Elrassi, Z. Capillary Zone Electrophoresis of Biological Substances with Fused-Silica Capillaries Having Zero or Constant Electroosmotic Flow. *Electrophoresis* **1993**, *14*, 396−406.

(29) Linder, V.; Verpoorte, E.; de Rooij, N. F.; Sigrist, H.; Thormann, W. Application of surface biopassivated disosable poly(dimethylsiloxane)/glass chips to a heterogeneous competitive human serum immunoglobulin G immunoassay with incorporated internal standard. *Electrophoresis* **2002**, *23*, 740−749.

(30) Johnson, T. J.; Ross, D.; Gaitan, M.; Locascio, L. E. Laser modification of preformed polymer microchannels: Application to reduce band broadening around turns subject to electrokinetic flow. *Anal. Chem.* **2001**, *73*, 3656−3661.

(31) Schasfoort, R. B. M.; Schlautmann, S.; Hendrikse, J.; van der Berg, A. Field Effect Flow Control for Microfabricated Fluidic Networks. *Science* **1999**, *286*, 942.

(32) Moorthy, J.; Khoury, C.; Moore, J. S.; Beebe, D. J. Active control of electroosmotic flow in microchannels using light. *Sens. Actuators, B* **2001**, *75*, 223−229.

(33) Ajdari, A. Electro-osmosis on inhomogeneously charged surfaces. *Phys. Rev. Lett.* **1995**, *75*, 755−758.

(34) Moorthy, J.; Khoury, C.; Stremler, M. A.; Moore, J. S.; Beebe, D. J. In *Technical Digest of the 2000 Solid-State and Actuator Workshop*, Hilton Head, SC, June 4-8, 2000.

(35) Erickson, D.; Li, D. Influence of Surface Heterogeneity on Electrokinetically Driven Microfluidic Mixing. *Langmuir* **2002**, *18*, 1883−1892.

(36) Ajdari, A. Transverse electrokinetic and microfluidic effects in micropatterned channels: Lubrication analysis for slab geometries. *Phys. Rev. E* **2002**, *6501*, art. no.-016301.

(37) Johnson, T. J., Ross, D., Locascio, L. E. Rapid Microfluidic Mixing. *Anal. Chem.* **2002**, *74*, 45−51.

(38) Stroock, A. D.; Dertinger, S. K. W.; Ajdari, A.; Mezic, I.; Stone, H. A.; Whitesides, G. M. Chaotic Mixer for Microchannels. *Science* **2002**, *295*, 647−651.

(39) Stroock, A. D.; Dertinger, S. K. W.; Whitesides, G. M.; Ajdari, A. Patterning Flows Using Grooved Surfaces. *Anal. Chem.* **2002**, *74*, 5306−5312.

(40) Liu, R. H.; Stremler, M. A.; Sharp, K. V.; Olsen, M. G.; Santiago, J. G.; Adrian, R. J.; Aref, H.; Beebe, D. J. Passive mixing in a three-dimensional serpentine microchannel. *J. Microelectromech. Syst.* **2000**, *9*, 190−197.

(41) Lemoff, A.; Lee, A. An AC Magnetohydrodynamic Micropump. *Sens. Actuators, B* **2000**, *63*, 178−185.

(42) Zhong, J. H.; Yi, M. Q.; Bau, H. H. Magneto hydrodynamic (MHD) pump fabricated with ceramic tapes. *Sens. Actuators, A* **2002**, *96*, 59−66.

(43) Bau, H. H.; Zhong, J. H.; Yi, M. Q. A minute magneto hydro dynamic (MHD) mixer. *Sens. Actuators, B* **2001**, *79*, 207−215.

(44) Handique, K.; Burke, D. T.; Mastrangelo, C. H.; Burns, M. A. Nanoliter liquid metering in microchannels using hydrophobic patterns. *Anal. Chem.* **2000**, *72*, 4100−4109.

(45) Zhao, B.; Moore, J. S.; Beebe, D. J. Surface-directed liquid flow inside microchannels. *Science* **2001**, *291*, 1023−1026.

(46) Chou, H. P.; Unger, M. A.; Quake, S. R. A Microfabricated Rotary Pump. *Biomed. Microdevices* **2001**, *3*, 323−330.

(47) Fuhr, G.; Schnelle, T.; Wagner, B. Travelling wave-driven microfabricated electrohydrodynamic pumps for liquids. *J. Micromech. Microeng.* **1994**, *4*, 217−226.

(48) Ajdari, A. Pumping liquids using asymmetric electrode arrays. *Phys. Rev. E* **2000**, *61*, R45−48.

(49) Brown, A. B. D.; Smith, C. G.; Rennie, A. R. Pumping of water with ac electric fields applied to asymmetric pairs of microelectrodes. *Phys. Rev. E* **2001**, *63*, 016305.

(50) Kenis, P. J. A.; Ismagilov, R. F.; Whitesides, G. M. Microfabrication inside Capillaries Using Multiphase Laminar Flow Patterning. *Science* **1999**, *285*, 83−85.

(51) Kenis, P. J. A.; Ismagilov, R. F.; Takayama, S.; Whitesides, G. M.; Li, S.; White, H. S. Fabrication Inside Microchannels using Fluid Flow. *Acc. Chem. Res.* **2000**, *33*, 841−847.

(52) Zhao, B.; Viernes, N. O. L.; Moore, J. S.; Beebe, D. J. Control and Applications of Immiscible Liquids in Microchannels. *J. Am. Chem. Soc.* **2002**, *124*, 5284−5285.

(53) Jeon, N. L.; Choi, I. S.; Xu, B.; Whitesides, G. M. Large-Area Patterning by Vacuum-Assisted Micromolding. *Adv. Mater.* **1999**, *11*, 946−950.

(54) Panwar, A. S.; Kumar, S. Brownian dynamics simulations of polymer stretching and transport in a complex electro-osmotic flow. *J. Chem. Phys.* **2003**, *118*, 925−936.

(55) Anderson, J. R.; Chiu, D. T.; Jackman, R. J.; Cherniavskaya, O.; McDonald, J. C.; Wu, H.; Whitesides, S. H.; Whitesides, G. M. Fabrication of Topologically Complex Three-Dimensional Microfluidic Systems in PDMS by Rapid Prototyping. *Anal. Chem.* **2000**, *72*, 3158−3164.

(56) Ottino, J. M. *The kinematics of Mixing: Stretching, Chaos, and Transport*; Cambridge University Press: Cambridge, 1989.

(57) We define the mixing length as the distance downstream that the solutions travel before they appear uniform in confocal images such as in Figure 4D.

(58) The diffusivity of the labeled polymer was measured to be $D = 2 \times 10^{-8}$ cm^2/s. The distance required to mix in a simple channel is estimated as, $\Delta y = U_a \Delta t_{mix}$, were U_a is the average axial flow speed, and $\Delta t_{mix} = (L/2)^2/4D$. L is the width of the channel. In the experiment shown in Figure 4D, $U_a \sim 1$ cm/s and $L = 200\ \mu$m, so $\Delta y \sim 10$ m.[38]

(59) Jones, S. W. The enhancement of mixing by chaotic advection. *Phys. Fluids A* **1991**, *3*, 1081−1086.

(60) Jeon, N. L.; Dertinger, S. K. W.; Chiu, D. T.; Choi, I. S.; Stroock, A. D.; Whitesides, G. M. Generation of Solution and Surface Gradients Using Microfluidic Systems. *Langmuir* **2000**, *16*, 8311−8316.

(61) Volpert, M.; Mezic, I.; Meinhart, C. D.; Dahleh, M. In *Proceedings of the First International Conference on Heat Transfer, Fluid Mechanics, and Thermodynamics*, Kruger Park, South Africa, April 8-10, 2002.

AR0202870